Progress In Electromagnetics Research Letters, Vol. 96, 7–15, 2021

Surface Mountable Compact Printed Dipole Antenna for GPS/WiMAX Applications

Hitesh Patel* **and Trushit Upadhyaya**

Abstract—A low-profile, electrically compact, and cost-effective antenna for wireless communication is presented. The antenna comprises self-complementary dipole elements on each side of the resonator surface. The dipole is excited using co-axial feed for an efficient impedance matching. An electrically compact antenna has dimensions of $0.13\lambda \times 0.26\lambda$ at the lower frequency. The dipole covers 1.57 GHz and 3.65 GHz frequencies offering the measured impedance bandwidth in the order of 1.83% and 2.30%, respectively. The self-complementary structure of the dipole having multiple coupling elements permits adequate tuning of the antenna on target frequencies. The resonant modes of the antenna can be tuned by merely modifying the position of the complementary structure on each side of the dipole. The engineered slots in the dipole permit further fine-tuning. The antenna presents gain in the order of 0.71 dBi and 1.27 dBi and stable radiation patterns for the two frequencies.

1. INTRODUCTION

The need for compact antennas is ever and rapidly growing in wireless communication devices. Wireless communication needs low-profile and cost-effective antenna solutions that can be swiftly integrated with circuit boards. Printed surface mountable antennas are optimum solutions to many challenges posed by compact communication devices. Dipole antenna offers all these abilities along with stable radiation characteristics. Printed dipole antennas can be integrated with communication devices offering single resonant modes to multiple resonant modes. Printed antennas are limited in terms of bandwidth and gain, however, offer ease in fabrication and device integration.

A systematic technique to engineer the surface-mountable antenna can be applied to achieve the target frequencies. Many works in literature present such techniques for dipole antennas [1–6]. The defected ground plane in surface-mountable antenna design is significantly useful for bandwidth optimization as extensively reported [7–11]. The defected ground plane technique does offer disadvantages of cross-polarization and front to back (F/B) ratio of the antenna. Due to simple design and compactness, printed antennas are tailored to achieve broadband characteristics using compound structures of dipole and monopole radiators [12–15]. The antennas for multiple resonances are quite famous in planar resonators. Such resonators are typically complex in nature and offer low operational bandwidth [16–19]. Loop-shaped resonators are widely utilized concepts for wireless devices. The literature offers a range of loop antennas designed for stable radiation characteristics [20–24]. Loop-shaped antenna, due to its nature of the shape, offers compactness in the design. By only modifying the number of loops, the effective electrical length of a loop antenna gets changed, and hence subsequently the antenna resonance can be altered.

The Split Ring Resonators (SRRs) are also widely utilized for antenna design compactness [25, 26]. Antenna compactness can be achieved by loading m-negative material in the antenna [27–29]. SRR has high Q-factor characteristics due to which the bandwidth of the excited resonance mode gets

Received 12 December 2020, Accepted 11 January 2021, Scheduled 22 January 2021
* Corresponding author: Hitesh Patel (hiteshpatel.ec@charusat.ac.in).
The authors are with the Charotar University of Science & Technology, Chnaga, Anand, Gujarat, India.

essentially limited. SRR array can be utilized for a strong electromagnetic response for the development of electrically compact resonators. The stability of the radiation characteristics of the antenna using m-negative material loading is a matter of concern. The slots in the patch are one of the easiest and stable techniques for antenna miniaturization. Slotted patch antenna is thus a widely utilized design for electrically small antennas. The presented design exploits the use of slotting on the patch and defected ground plane for achieving the target dual-band resonance at GPS and WiMAX frequencies. The open-ended slots of the proposed antenna provide wide impedance bandwidth. The dimensions and positions of the open-ended slots are varied for meeting the target resonance frequencies.

2. ANTENNA CONFIGURATION

The antenna was designed in a finite element analysis based software simulator. The dipole was fabricated on standard FR-4 laminate. The dimensions of the selected substrate of the antenna are $25\,\text{mm} \times 50\,\text{mm}$ which is $0.13\lambda \times 0.26\lambda$ at the lower frequency. The electrical dimensions of the antenna are quite compact. The height of the substrate is selected as 1.56 mm. The FR4 provides a cost-effective solution in the case of mass-production of the PCBs; however while being utilized for high-frequency spectrum regimes, it introduces quite high losses due to its high loss tangent around 0.02. This reduces the radiation properties of the antenna, and especially the antenna gain gets reduced due to induced dielectric losses. It is recommended to use a low-loss material for designing the antennas for high-frequency applications; however, these laminates come with a higher cost.

The slots in the antenna alter the electrical length of the resonator and thus alters the resonance. Figure 1 depicts the proposed dipole antenna. Typically, such dipole and monopole antennas are fed with a microstrip line; in this design, coaxial cable excitation is provided to optimize the impedance matching. The location of the SMA connector is also optimized manually by taking multiple iterations in the numerical simulation. A gold-plated SMA connector is used to further reduce the losses. The induced surface current density on the top of the patch excites the resonant modes. Due to the symmetrical structure, there shall be symmetrical induced currents on the slotted lines of the resonator.

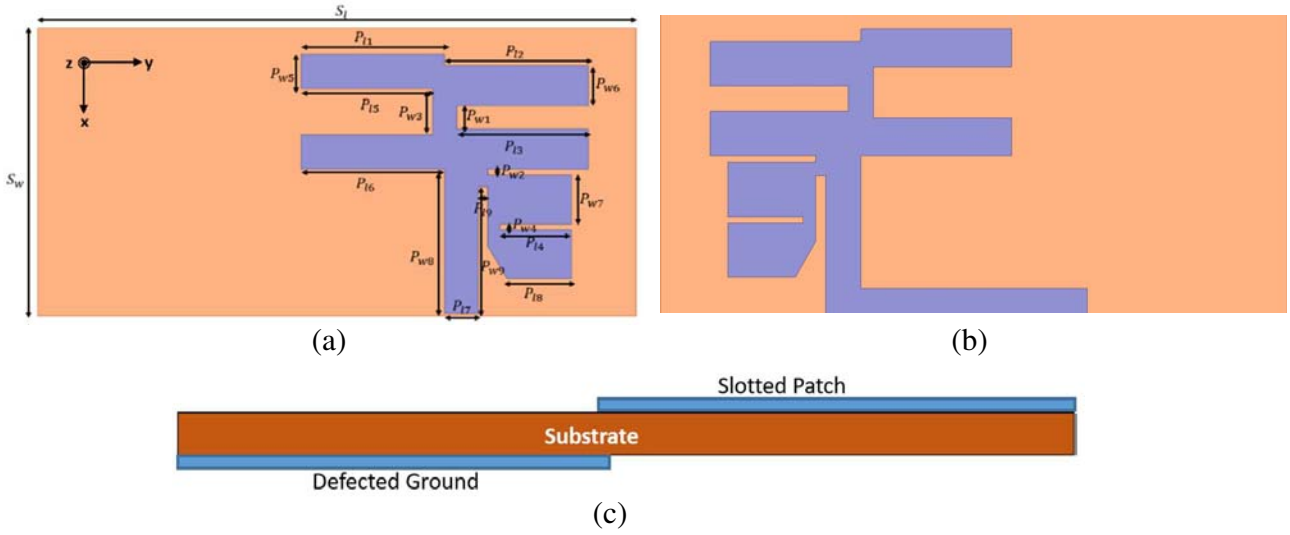

Figure 1. Antenna views. (a) Top, (b) bottom, (c) perspective.

In addition, impedance bandwidth can be swiftly improved by further tweaking of the leveled arms of the resonators. The strip extension to the slotted dipole allows the smooth mode transition from the line to the slotted strips. The gap between the slotted flares of the dipole is iteratively modified to optimize the performance of the patch resonator. The balanced feeding is apparently due to the structural symmetry. The utilization of the coaxial feeding along with reflected conducting sheet beneath the coaxial connector matching real-time connector caused the feeding impedance to be exactly

50 Ω. The presented antenna exhibits two resonant modes excited for GPS and WiMAX applications. The dimensions in mm are $S_W = 25$, $S_L = 50$, $P_{l1} = 12$, $P_{l2} = 12$, $P_{l3} = 11$, $P_{l4} = 5$, $P_{l5} = 11$, $P_{l6} = 12$, $P_{l7} = 2.8$, $P_{l8} = 5.38$, $P_{l9} = 0.2$, $P_{w1} = 2$, $P_{w2} = 0.5$, $P_{w3} = 4$, $P_{w4} = 0.5$, $P_{w5} = 3$, $P_{w6} = 3.5$, $P_{w7} = 4.25$, $P_{w8} = 12.5$, $P_{w9} = 11$.

3. RESULTS AND DISCUSSION

The proposed dipole was simulated using High Frequency Structure Simulator. A prototype was developed to measure the results achieved through software numerical simulations. The fabricated module is presented in Figure 2. Keysight tabletop network analyzer, N9912A, was utilized for the measurement of the reflection coefficient. The simulated and measured reflection coefficients are represented in Figure 3. The antenna has resonant frequencies of 1.575 GHz and 3.65 GHz. As apparent from the figure, measured return loss values are around 14.08 and 15.92 at 1.575 GHz and 3.65 GHz frequencies. This makes the Voltage Standing Wave Ratio (VSWR) around 1.49 and 1.38 for respective frequencies. These VSWR values are less than 1.5 as per the typical required real-time values for antenna modules. The slight variation in the return loss in measured values compared to the simulated values of return loss is due to fine mechanical inaccuracies. The antenna has good measured impedance bandwidth of 1.83% at 1.575 GHz and 2.30% at 3.65 GHz. Table 1 shows antenna radiation characteristics.

The surface current density distribution of the presented dipole is depicted in Figure 4. The maxima for 1.575 GHz is visible near the strip along with the feed and gaps. The concentric coupling gives rise to the mode being excited. For the 3.65 GHz frequency, the current density distribution is continuous on vertical pole. The induced field is stronger in case of 3.65 GHz than 1.575 GHz frequency.

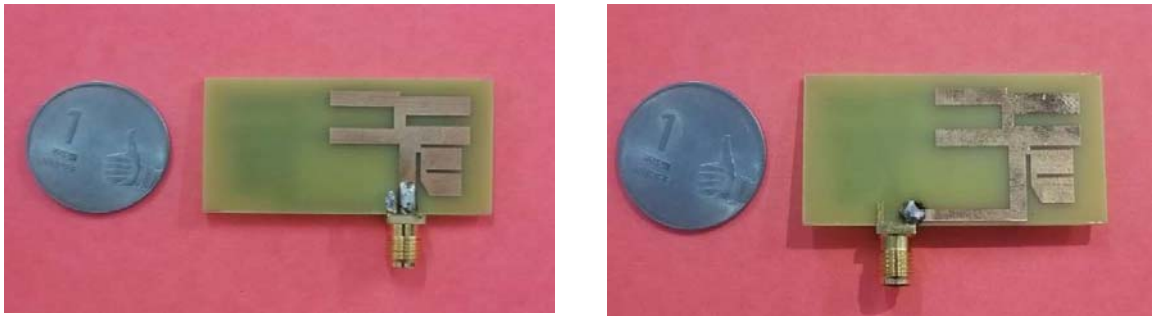

(a) (b)

Figure 2. Fabricated prototype. (a) Top view, (b) bottom view.

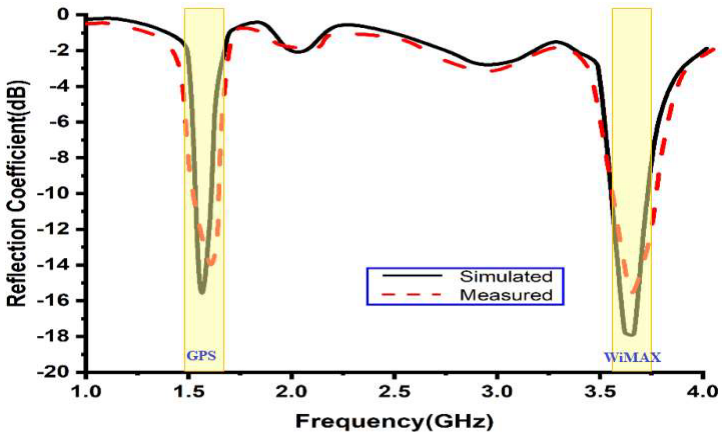

Figure 3. Reflection coefficient of the antenna (Dashed: measured, continuous: simulated).

Table 1. Antenna radiation characteristics.

Antenna Parameters	First Frequency Band Simulated/Measured	Second Frequency Band Simulated/Measured
Resonance	1.569 GHz/1.572 GHz	3.635 GHz/3.65 GHz
Reflection Coefficient	−15.89 dB/−14.08 dB	−18.86 dB/−15.92 dB
Impedance Bandwidth	1.53%/1.83%	2.48%/2.30%
Peak Gain	1.38 dBi/0.71 dBi	4.01 dBi/3.75 dBi

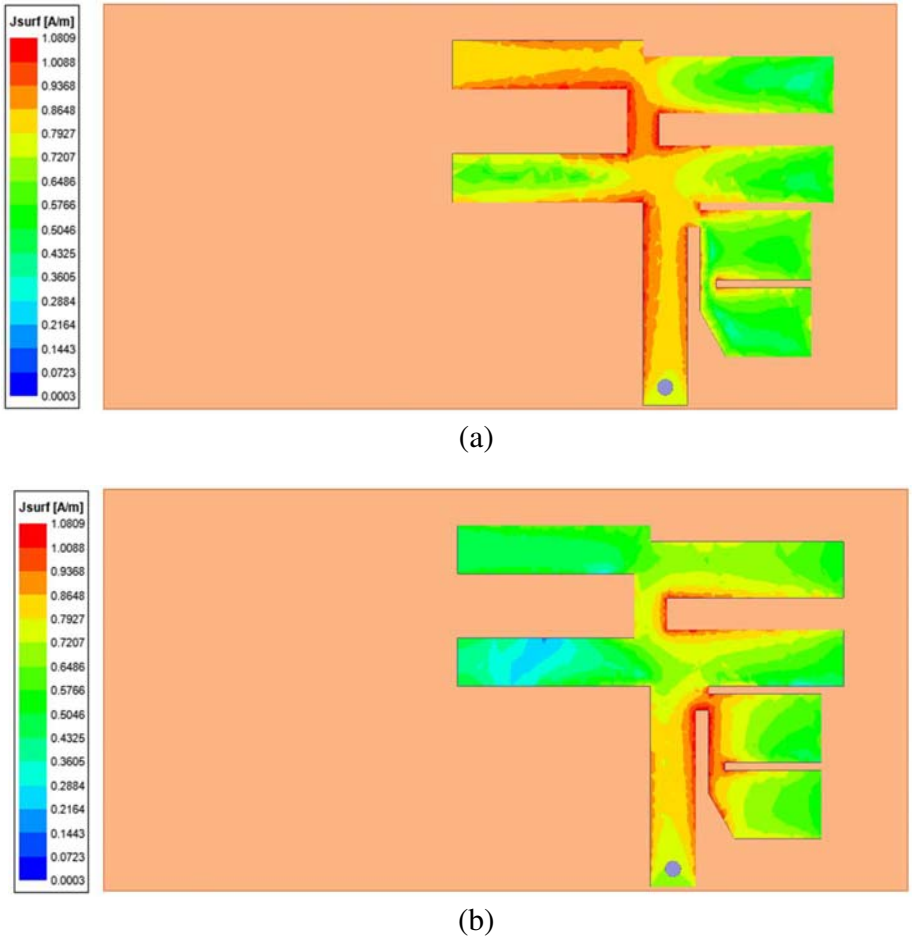

Figure 4. Antenna current distribution (a) 1.575 GHz, (b) 3.65 GHz.

Several dimensions of the dipole strips and gaps are varied as demonstrated in Figure 5. The mutual coupling between the strips can cause the alteration in effective impedance and capacitance of the dipole resonator. The mutual coupling between two elements looks very strong for the short bottom right arm and strip connected near the feed. As a consequence, the interaction between fields contributed from these two arms shall have distinct effects. In Figure 5(a), the length of upper-right arm P_{l3} is varied to see the variations in the return loss characteristics. The second resonance had significant variation while the modification in P_{l3} was carried out. The variation in lower arm length P_{l4} caused shift in the resonance for both the frequencies as in Figure 5(b). The same is true for Figure 5(c). The change in the value of reflection coefficient was noticed when the widths of the arms were modified. Figures 5(d) through 5(f) depict return losses when the distances between two arms were altered. A plane rectangle

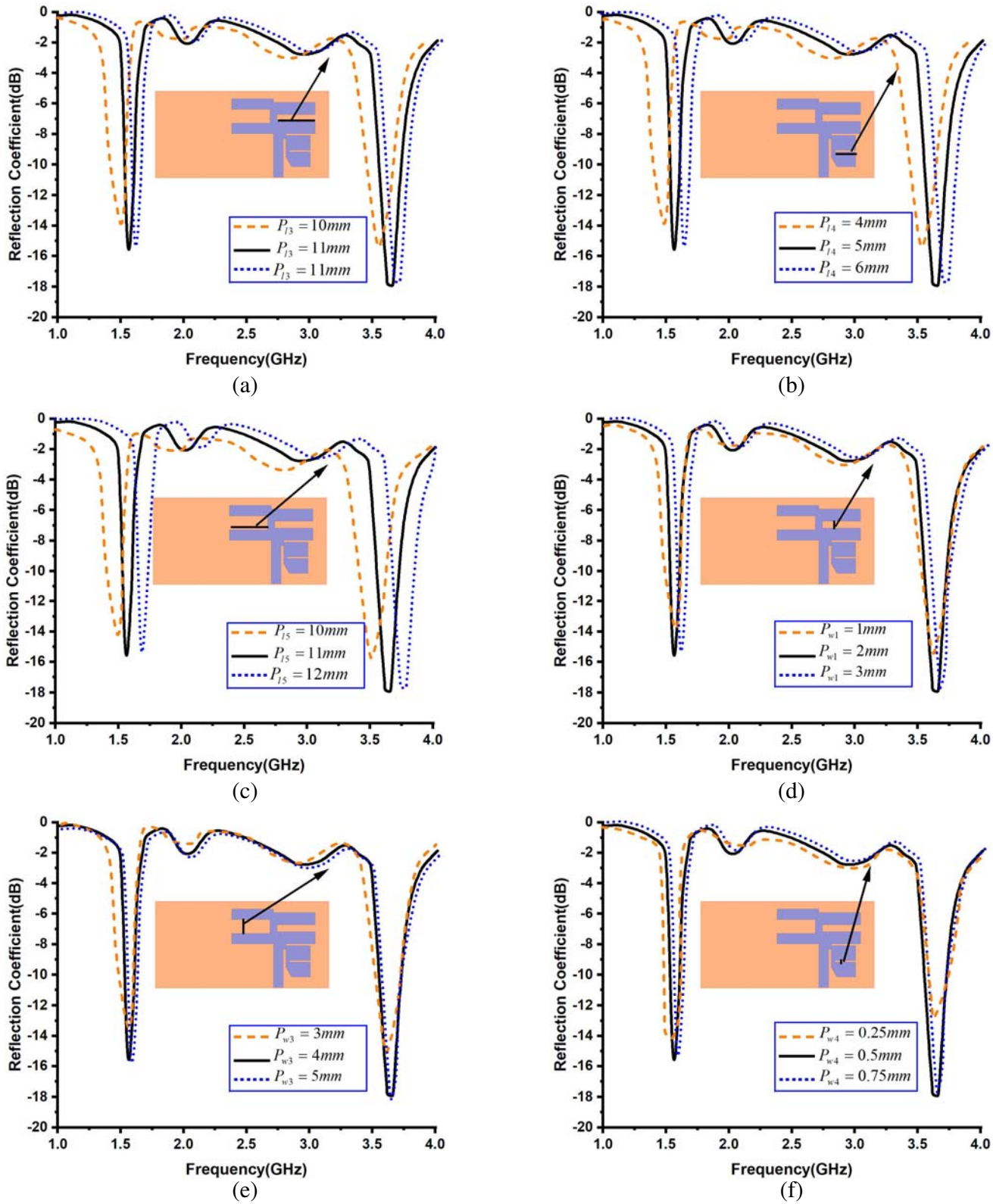

Figure 5. Parametric variations (a) P_{l3}, (b) P_{l4}, (c) P_{l5}, (d) P_{w1}, (e) P_{w3}, (f) P_{w4}.

monopole was designed for meeting the target frequency. However, the dimensions of these monopole were quite higher than the proposed design. The slits were introduced one by one for meeting the typical criteria of resonance frequency, desired bandwidth, and the gain. Subsequently as presented in Figure 5, multiple iterations were carried out through software numerical solutions. The presented antenna shows the optimized dimension of the monopole.

The radiation patterns were measured in a shielded anechoic chamber as pictured in Figure 6. The chamber provides the isolation around 25 dB for the measured frequencies. The dimensions of the anechoic chamber were $3 \times 3 \times 3\,\mathrm{m}^3$. The horn antenna in the anechoic chamber was excited to measure the radiation pattern. The measured pattern was simulated in a commercial tool built upon MATLAB software. Ultra low-lossy cables were employed for the connection from Horn to VNA and antenna to VNA to minimize cable losses. Both E-field and H-field patterns were measured in the shielded anechoic chamber. The material of the turntable is designed in such a way to reduce the reflections at these frequencies. The numerical simulated and measured radiation patterns at both target frequencies are depicted in Figure 7. As expected, a figure-of-eight pattern appears for the proposed dipole. The antenna has electrical tilt due to its virtue of shape. The slots in the dipole modify the surface current directions and subsequently the current density on the resonator. The field emitting from these resonators shall essentially be electrically tilted as in E-Field patterns of the antenna. The

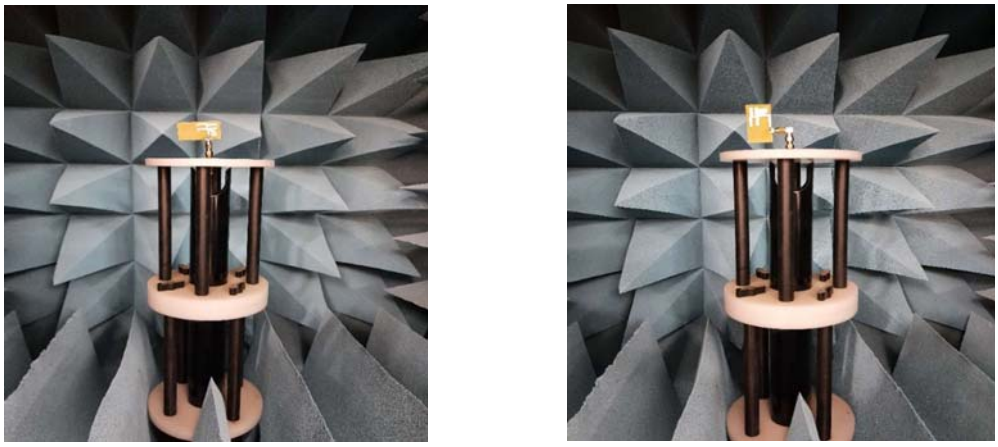

(a) (b)

Figure 6. Measurement in anechoic chamber.

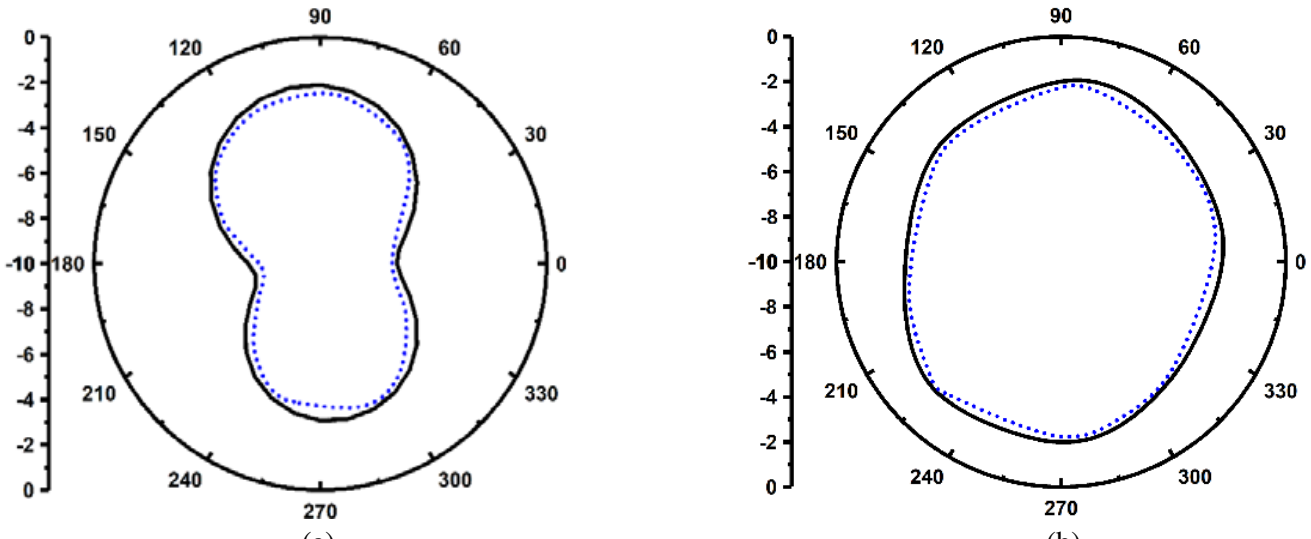

(a) (b)

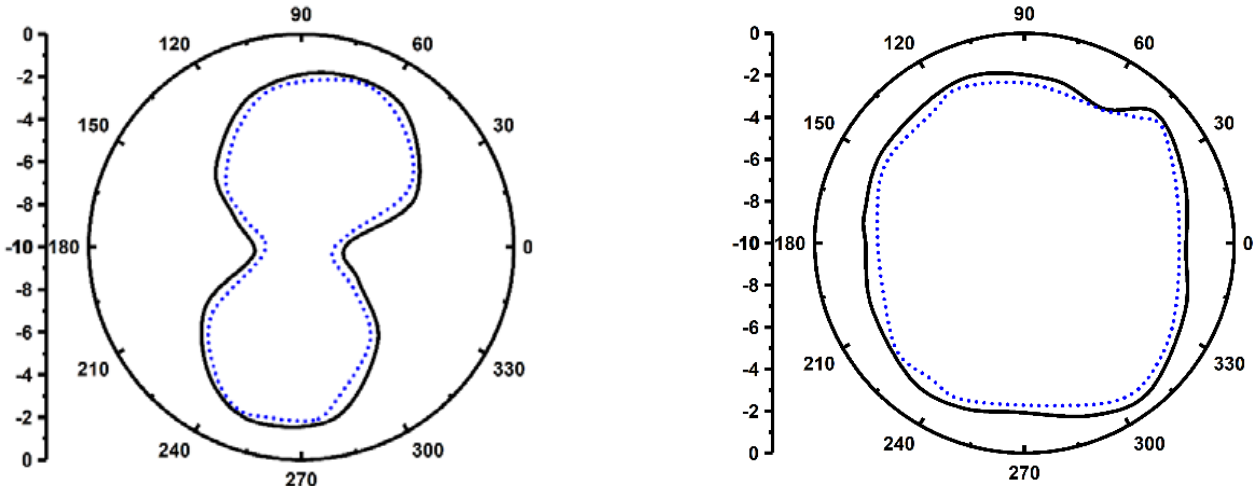

Figure 7. Radiation patterns (a) E-plane (y-z plane) at 1.575 GHz, (b) H-plane (x-z plane) at 1.575 GHz, (c) E-plane (y-z plane) at 3.65 GHz, (d) H-plane (x-z plane) at 3.65 GHz.

Table 2. Comparison of antenna with designs available in literature.

Citation	Frequency (GHz)	Gain (dBi)	Bandwidth (%)	Antenna Dimension (mm^3)
[14]	2.4, 2.59, 2.95, 3.7, 4.12, 4.5, 5.5	1.89, 1.61, 0.97, 0.98, 1.72, 1.92	14.16, 6.78, 6.21, 3.15, 7.77, 8.18	$50 \times 200 \times 1.6$
[30]	1.57, 1.85, 2.44	-1, 0, 0.2	0.8, 0.5, 0.8	$41.1 \times 45.5 \times 0.8$
[31]	2.4, 3.5, 5	4.5, 4.2, 5.1	12.2, 5.6, 7.6	$75 \times 75 \times 1.6$
Proposed	1.57, 3.65	0.71, 1.27	1.83, 2.30	$25 \times 50 \times 1.56$

H-field pattern of the dipole resonator is typically circular. Figure 8 depicts the antenna gain and radiation efficiency plots. The antenna efficiencies were in order of 61% and 75% for 1.575 GHz and 3.65 GHz, respectively. The efficiency may be further improved by employing tapered-line from coaxial feed to the dipole resonator.

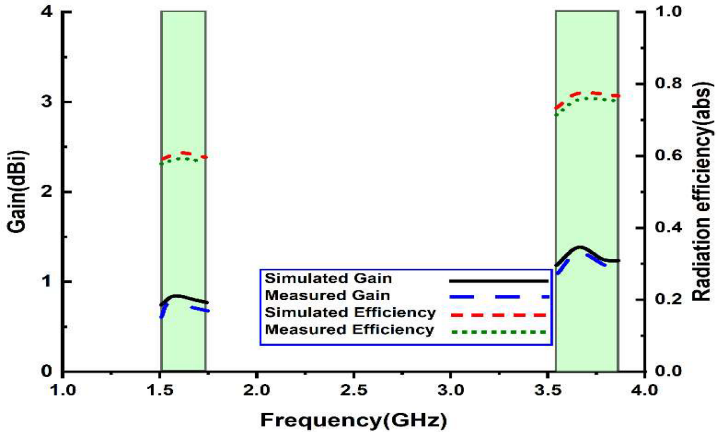

Figure 8. Antenna gain and radiation efficiency.

The proposed antennas exhibit benefit either in terms of gain or bandwidth or antenna dimensions as shown in the comparison in Table 2.

4. CONCLUSION

A planar dual-band dipole antenna was designed for 1.575 GHz and 3.65 GHz frequency bands targeting GPS and WiMAX operations. The dipole provides good bandwidth around 1.83% and 2.30% for these frequencies, respectively. The antenna exhibits a stable radiation pattern with satisfactory gain in order of 0.71 dBi and 1.27 dBi. The measured results have close correlation with the simulated ones which shows employability of the proposed antenna in a communication module.

REFERENCES

1. Takeshore, K., S. Singh, C. Sairam, and S. D. Ahirwar, "Design of asymmetric wideband printed dipole antenna using inset feeding technique," *Progress In Electromagnetics Research C*, Vol. 96, 87–96, 2019.
2. Kedze, K. E., H. Wang, S. X. Ta, and I. Park, "Wideband low-profile printed dipole antenna incorporated with folded strips and corner-cut parasitic patches above the ground plane," *IEEE Access*, Vol. 7, 15537–15546, 2019.
3. Singh, A., J. Meena, N. Baghel, and S. Mukherjee, "Design of printed dipole antenna for enhanced coverage efficiency," *2020 URSI Regional Conference on Radio Science (URSI-RCRS)*, 1–6, IEEE, February 2020.
4. Ma, T. G. and S. K. Jeng, "A printed dipole antenna with tapered slot feed for ultrawide-band applications," *IEEE Transactions on Antennas and Propagation*, Vol. 53, No. 11, 3833–3836, 2005.
5. Liu, N. W., L. Zhu, W. W. Choi, and X. Zhang, "Wideband shorted patch antenna under radiation of dual-resonant modes," *IEEE Transactions on Antennas and Propagation*, Vol. 65, No. 6, 2789–2796, 2017.
6. Qu, S. W., J. L. Li, Q. Xue, and C. H. Chan, "Wideband periodic endfire antenna with bowtie dipoles," *IEEE Antennas and Wireless Propagation Letters*, Vol. 7, 314–317, 2008.
7. Khandelwal, M. K., B. K. Kanaujia, and S. Kumar, "Defected ground structure: Fundamentals, analysis, and applications in modern wireless trends," *International Journal of Antennas and Propagation*, 2017.
8. Patel, U. P. and T. K. Upadhyaya, "Design and analysis of compact μ-negative material loaded wideband electrically compact antenna for WLAN/WiMAX applications," *Progress In Electromagnetics Research M*, Vol. 79, 11–22, 2019.
9. Kishore, N., A. Prakash, and V. S. Tripathi, "A reconfigurable ultra wide band antenna with defected ground structure for ITS application," *AEU-International Journal of Electronics and Communications*, Vol. 72, 210–215, 2017.
10. Singhal, S. and A. K. Singh, "Asymmetrically CPW-fed hourglass shaped UWB monopole antenna with defected ground plane," *Wireless Personal Communications*, Vol. 94, No. 3, 1685–1699, 2017.
11. Zeng, J. and K. M. Luk, "A simple wideband magnetoelectric dipole antenna with a defected ground structure," *IEEE Antennas and Wireless Propagation Letters*, Vol. 17, No. 8, 1497–1500, 2018.
12. Upadhyaya, T. K., A. Desai, and R. H. Patel, "Design of printed monopole antenna for wireless energy meter and smart applications," *Progress In Electromagnetics Research Letters*, Vol. 77, 27–33, 2018.
13. Tseng, C. F. and C. L. Huang, "A wideband cross monopole antenna," *IEEE Transactions on Antennas and Propagation*, Vol. 57, No. 8, 2464–2468, 2009.
14. Patel, H. and T. K. Upadhyaya, "Printed multiband monopole antenna for smart energy meter/WLAN/WiMAX applications," *Progress In Electromagnetics Research M*, Vol. 89, 43–51, 2020.

15. Shuai, C. Y. and G. M. Wang, "A novel planar printed dual-band magneto-electric dipole antenna," *IEEE Access*, Vol. 5, 10062–10067, 2017.
16. Liu, N. W., L. Zhu, W. W. Choi, and X. Zhang, "A low-profile aperture-coupled microstrip antenna with enhanced bandwidth under dual resonance," *IEEE Transactions on Antennas and Propagation*, Vol. 65, No. 3, 1055–1062, 2017.
17. Upadhyaya, T., A. Desai, R. Patel, U. Patel, K. P. Kaur, and K. Pandya, "Compact transparent conductive oxide based dual band antenna for wireless applications," *2017 Progress In Electromagnetics Research Symposium — Fall (PIERS — FALL)*, 41–45, Singapore, Nov. 19–22, 2017.
18. Lu, W. J., Q. Li, S. G. Wang, and L. Zhu, "Design approach to a novel dual-mode wideband circular sector patch antenna," *IEEE Transactions on Antennas and Propagation*, Vol. 65, No. 10, 4980–4990, 2017.
19. Patel, R., T. Upadhyaya, and A. Desai, "Capacitive couplings compact antenna for LTE/WiMAX/WLAN application," *Microwave and Optical Technology Letters*, Vol. 60, No. 12, 2977–2983, 2018.
20. Rezaeieh, S. A. and A. M. Abbosh, "Compact planar loop-dipole composite antenna with director for bandwidth enhancement and back radiation suppression," *IEEE Transactions on Antennas and Propagation*, Vol. 64, No. 8, 3723–3728, 2016.
21. Zahid, M. N., J. Jiang, U. Rafique, and D. Eric, "Modified planar square-loop antenna for electronic article surveillance radio frequency identification applications," *Journal of Communications Technology and Electronics*, Vol. 65, No. 10, 1161–1166, 2020.
22. Lu, W. J., G. M. Liu, K. F. Tong, and H. B. Zhu, "Dual-band loop-dipole composite unidirectional antenna for broadband wireless communications," *IEEE Transactions on Antennas and Propagation*, Vol. 62, No. 5, 2860–2866, 2014.
23. Rezaeieh, S. A., A. Zamani, K. S. Bialkowski, and A. M. Abbosh, "Unidirectional slot-loaded loop antenna with wideband performance and compact size for congestive heart failure detection," *IEEE Transactions on Antennas and Propagation*, Vol. 63, No. 10, 4557–4562, 2015.
24. Khanjari, S. P., S. Jarchi, and M. Mohammad-Taheri, "Compact and wideband planar loop antenna with microstrip to parallel strip balun feed using metamaterials," *AEU-International Journal of Electronics and Communications*, Vol. 111, 152883, 2019.
25. Upadhyaya, T. K., S. P. Kosta, R. Jyoti, and M. Palandoken, "Negative refractive index material-inspired 90-deg electrically tilted ultra wideband resonator," *Optical Engineering*, Vol. 53, No. 10, 107104, 2014.
26. Kedze, K. E., H. Wang, and I. Park, "Compact broadband omnidirectional radiation pattern printed dipole antenna incorporated with split-ring resonators," *IEEE Access*, Vol. 6, 49537–49545, 2018.
27. Upadhyaya, T. K., S. P. Kosta, R. Jyoti, and M. Palandöken, "Novel stacked μ-negative material-loaded antenna for satellite applications," *International Journal of Microwave and Wireless Technologies*, Vol. 8, No. 2, 229, 2016.
28. Desai, A. and T. Upadhyaya, "Transparent dual band antenna with μ-negative material loading for smart devices," *Microwave and Optical Technology Letters*, Vol. 60, No. 11, 2805–2811, 2018.
29. Geetharamani, G. and T. Aathmanesan, "A metamaterial inspired tapered patch antenna for WLAN/WiMAX applications," *Wireless Personal Communications*, 1–13, 2020.
30. Wang, Y. D., J. H. Lu, and H. M. Hsiao, "Novel design of semi-circular slot antenna with triple-band operation for WLAN/WIMAX communication," *Microwave and Optical Technology Letters*, Vol. 50, No. 6, 1531–1534, 2008.
31. Azaro, R., E. Zeni, P. Rocca, and A. Massa, "Innovative design of a planar fractal-shaped GPS/GSM/Wi-Fi antenna," *Microwave and Optical Technology Letters*, Vol. 50, No. 3, 825–829, 2008.